https://doi.org/10.3311/PPee.20048

Periodica Polytechnica Electrical Engineering and Computer Science, 66(2), pp. 139–147, 2022

Predictive-DPC Based on Duty Cycle Control of PWM Rectifier under Unbalanced Network

Tarik Mohammed Chikouche[1*], Kada Hartani[1], Tahar Terras[1]

[1] Electrotechnical Engineering Laboratory, Electrotechnical Department, Faculty of Technology, University of Saida Dr. Moulay Tahar, P. O. B. 138, 20000 Ennasr, Saida, Algeria
[*] Corresponding author, e-mail: chikouche.tarik@univ-saida.dz

Received: 23 February 2022, Accepted: 11 April 2022, Published online: 28 April 2022

Abstract

This work proposes a predictive direct power control (P-DPC) technique of a PWM rectifier, based on a duty cycle control method, using a new definition of the instantaneous reactive power in the predefined cost function, able to operate under balanced and unbalanced grid voltages. In conventional DPC, the use of a single voltage vector during a control period leads to high power ripples and variable switching frequency. To overcome these problems, a duty cycle control is introduced in P-DPC to achieve performance improvement in terms of power ripple reduction, dynamic response and robustness against unbalanced grid voltages. Its main characteristic is the use of several voltage vectors applied during a control period. In effect, the duration of the selected vector is determined by minimizing the active power ripple during a control period. Simulation results are presented to confirm the theoretical study developed.

Keywords

predictive direct power control, duty cycle control, PWM rectifier, unbalanced network, power quality

1 Introduction

The use of PWM rectifiers in grid-connected power conversion systems has grown rapidly over the past decades, especially in applications of variable speed wind turbine generators, motor drives requiring regenerative capability, decentralized production systems, micro-grids, ultra-fast battery chargers for electric vehicles, etc. [1–3]. Therefore, more stringent requirements are placed on PWM rectifiers, especially when grid voltages are unbalanced, which is very common in rural areas with weak grids [4, 5].

The most popular research approach for controlling PWM rectifiers under balanced grid voltages is voltage oriented control (VOC) [6]. Many works have been done based on VOC to eliminate harmonic currents and DC bus voltage oscillations under unbalanced network. The disadvantage of this method is the setting of the internal current controllers and the strong dependence on system parameters [7]. Using a modification of Voltage Oriented Control (VOC) based on Dual Vector Current Controllers (DVCC) and Phase Locked Loops (PLL), Bobrowska-Rafał et al. [8] studied control structure for three-phase two-level PWM rectifier under unbalanced grid voltage conditions. The performance of the double synchronous reference frame controller is investigated in [9, 10], and its structure is improved by the addition of a decoupling network for estimating and mitigating undesired current oscillations.

Recently, the direct power control (DPC) is another high-performance control approach for PWM rectifiers. Compared to VOC, the DPC directly selects the desired voltage vector from a predefined switching table to regulate active and reactive powers [11]. Despite its advantages in terms of simple structure, high performance control which offers a unit power factor and a low rate of harmonic distortion of the currents absorbed, DPC has large steady-state power ripples and a variable switching frequency. Recent works on the DPC try to overcome these drawbacks. Chikouche and Hartani [12] proposed a new switching table to enhance the DPC of three-phase PWM rectifiers and achieve higher performance in terms of power ripple reduction and dynamic response. Predictive-DPC of three-phase PWM rectifier using space-vector modulation (SVM) is developed in [13] without using predefined switching table and voltage vector. The concept of duty cycle control is introduced in DPC by [14, 15], which allocates just a fraction of the control period to the voltage vector selected from the standard switching table in DPC, while a zero vector is used for the rest of time.

Cite this article as: Mohammed Chikouche, T., Hartani, K., Terras, T. "Predictive-DPC Based on Duty Cycle Control of PWM Rectifier under Unbalanced Network", Periodica Polytechnica Electrical Engineering and Computer Science, 66(2), pp. 139–147, 2022. https://doi.org/10.3311/PPee.20048

The VOC control method used in [16] provides a new definition of instantaneous reactive power more appropriate for unbalanced grid voltages which requires positive/negative sequence extraction of grid voltages/currents and complicated control. Currently, only a few works have addressed the problem of DPC control of PWM rectifiers under unbalanced network voltages. Chikouche et al. [17] proposed an improved DPC control technique when grid voltages are unbalanced using a new definition of instantaneous reactive power without resorting to complicated sequence extraction. Predictive-DPC has been offered recently as a powerful alternative to conventional DPC, because it is more precise and successful in vector selection [18]. Selecting a better voltage vector by minimizing a cost function consisting of power errors, provides better steady-state performance in terms of power ripples and harmonic currents can be obtained. However, because only one voltage vector is applied during the control period, the sampling frequency must be high [19]. The duty cycle control method was introduced in DPC to improve steady state performance [14, 20, 21]. For example, the principle of active power ripple minimization is used to determine the duration of the selected vector from the switching table defined in the DPC [17]. This paper proposes an improvement by replacing vector selection with the cost function minimization principle in predictive direct power control (P-DPC).

The goal of this study is to improve P-DPC's ability to operate under unbalanced grid voltages while maintaining its conceptual simplicity and fast response. We are developing a new control method, as an alternative to the conventional DPC control, called the "Predictive direct power control integrating the duty cycle control". Its main characteristic is the use of several voltage vectors applied during a control period. In this studied control method, a duty cycle control method is applied to the output vector of the P-DPC control.

The remainder of the paper is organized as follows. In Section 2, a modeling of the two-level PWM rectifier power circuit under the conditions of unbalanced network voltages was presented. In Section 3, a predictive direct power control (P-DPC) based on duty cycle control is proposed for the control of three-phase two-level PWM rectifier. Firstly, to predict the future value of active power and new reactive power under unbalanced grid voltages, a suitable mathematical model is established and analyzed in detail. Active power and new reactive power are controlled simultaneously using a single cost function. Secondly, a duty cycle control technique is introduced to the predictive direct power control (P-DPC) to select an active vector and a zero vector during a control period. A detailed comparative study of conventional DPC and P-DPC integrating duty cycle control is carried out. Simulation and conclusive remarks are presented in Section 4 followed by a final Conclusion.

2 PWM rectifier model under an unbalanced network

Fig. 1 shows the power structure of three-phase PWM rectifier [17, 22].

The mathematical model of the PWM rectifier in the $\alpha\beta$ frame is expressed by

$$e_{\alpha\beta} = Ri_{\alpha\beta} + L\frac{di_{\alpha\beta}}{dt} + v_{\alpha\beta}, \tag{1}$$

where $v_{\alpha\beta}$, $e_{\alpha\beta}$ and $i_{\alpha\beta}$ are voltage vector components of the PWM rectifier, voltage vector of the grid and current vector of the grid. R and L are resistance and inductance of smoothing inductor.

The complex power S on the grid side can be given as

$$S = \frac{3}{2}\left(i^*_{\alpha\beta} e_{\alpha\beta}\right) = P + jQ, \tag{2}$$

where "*" denotes the conjugate of a complex vector.

Voltages and currents can be represented as the sum of their respective positive sequence and negative sequence vectors in unbalanced network conditions, as

$$e_{\alpha\beta} = e^+_{dq} e^{j\omega t} + e^-_{dq} e^{-j\omega t} = e^+_{\alpha\beta} + e^-_{\alpha\beta} \tag{3}$$

$$i_{\alpha\beta} = i^+_{dq} e^{j\omega t} + i^-_{dq} e^{-j\omega t} = i^+_{\alpha\beta} + i^-_{\alpha\beta}. \tag{4}$$

The active and reactive power can be described as follows:

$$P = \mathrm{Re}(S) = \frac{3}{2}\mathrm{Re}\left(i^*_{\alpha\beta} e_{\alpha\beta}\right) \tag{5}$$

$$Q = \mathrm{Im}(S) = \frac{3}{2}\mathrm{Im}\left(i^*_{\alpha\beta} e_{\alpha\beta}\right). \tag{6}$$

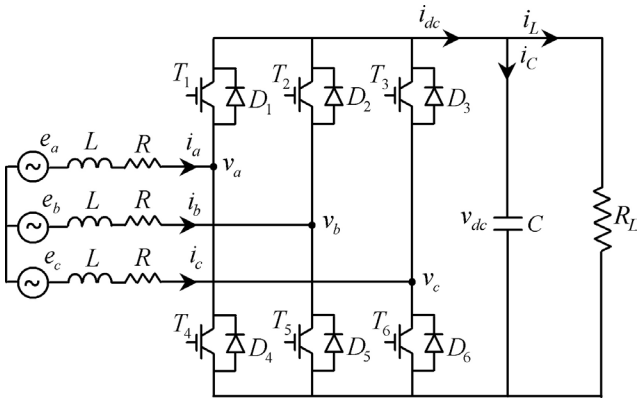

Fig. 1 Power structure of three-phase PWM rectifier

The new definition of reactive power is described as

$$Q^{nov} = \frac{3}{2}\mathrm{Re}\left(i^{*}_{\alpha\beta} e'_{\alpha\beta}\right). \tag{7}$$

The delayed phase value of the unbalanced network voltage can be described as

$$\begin{aligned} e'_{\alpha\beta} &= e^{+}_{dq} e^{j\left(\omega t-\frac{\pi}{2}\right)} + e^{-}_{dq} e^{-j\left(\omega t-\frac{\pi}{2}\right)} \\ &= -je^{+}_{dq} e^{j\omega t} + je^{-}_{dq} e^{-j\omega t} = -je^{+}_{\alpha\beta} + je^{-}_{\alpha\beta}. \end{aligned} \tag{8}$$

Active power and new reactive power can be expressed as in the case of unbalanced networks:

$$\begin{aligned} P &= \frac{3}{2}\mathrm{Re}\left[\left(i^{+}_{dq} e^{j\omega t} + i^{-}_{dq} e^{-j\omega t}\right)^{*}\left(e^{+}_{dq} e^{j\omega t} + e^{-}_{dq} e^{-j\omega t}\right)\right] \\ &= P_0 + P_{c2}\cos(2\omega t) + P_{s2}\sin(2\omega t) \end{aligned} \tag{9}$$

$$\begin{aligned} Q^{nov} &= \frac{3}{2}\mathrm{Re}\left[\left(i^{+}_{dq} e^{j\omega t} + i^{-}_{dq} e^{-j\omega t}\right)^{*}\left(-je^{+}_{dq} e^{j\omega t} + je^{-}_{dq} e^{-j\omega t}\right)\right] \\ &= Q^{nov}_0 + Q^{nov}_{c2}\cos(2\omega t) + Q^{nov}_{s2}\sin(2\omega t), \end{aligned} \tag{10}$$

where:

$$\begin{cases} P_0 = \frac{3}{2}\left(i^{+}_{dq} \bullet e^{+}_{dq} + i^{-}_{dq} \bullet e^{-}_{dq}\right) \\ P_{c2} = \frac{3}{2}\left(i^{+}_{dq} \bullet e^{-}_{dq} + i^{-}_{dq} \bullet e^{+}_{dq}\right) \\ P_{s2} = \frac{3}{2}\left(i^{+}_{dq} \otimes e^{-}_{dq} - i^{-}_{dq} \otimes e^{+}_{dq}\right) \\ Q^{nov}_0 = \frac{3}{2}\left(i^{+}_{dq} \otimes e^{+}_{dq} - i^{-}_{dq} \otimes e^{-}_{dq}\right) \\ Q^{nov}_{c2} = \frac{3}{2}\left(-i^{+}_{dq} \otimes e^{-}_{dq} + i^{-}_{dq} \otimes e^{+}_{dq}\right) \\ Q^{nov}_{s2} = \frac{3}{2}\left(i^{+}_{dq} \bullet e^{-}_{dq} + i^{-}_{dq} \bullet e^{+}_{dq}\right) \end{cases}. \tag{11}$$

From Eqs. (3) and (8), the derivatives of the network voltage vector and its lagged value can be obtained as follows:

$$\frac{de_{\alpha\beta}}{dt} = j\omega e^{+}_{\alpha\beta} - j\omega e^{-}_{\alpha\beta} = -\omega e'_{\alpha\beta} \tag{12}$$

$$\frac{de'_{\alpha\beta}}{dt} = \omega e^{+}_{\alpha\beta} + \omega e^{-}_{\alpha\beta} = \omega e_{\alpha\beta}\,. \tag{13}$$

From Eq. (1), the derivative of the network current can be expressed as

$$\frac{di_{\alpha\beta}}{dt} = \frac{1}{L}\left(e_{\alpha\beta} - v_{\alpha\beta} - Ri_{\alpha\beta}\right). \tag{14}$$

Substituting Eqs. (12) and (13) in Eq. (5) and considering Eq. (7), the derivative of the active power can be obtained as follows:

$$\frac{dP}{dt} = \frac{3}{2L}\left[\left|e_{\alpha\beta}\right|^2 - \mathrm{Re}\left(v^{*}_{\alpha\beta} \times e_{\alpha\beta}\right)\right] - \frac{R}{L}P - \omega Q^{nov}. \tag{15}$$

Similarly, the derivative of reactive power can be obtained from Eqs. (7), (12), (13) and (14) as

$$\frac{dQ^{nov}}{dt} = \frac{3}{2L}\mathrm{Re}\left[\left(e^{*}_{\alpha\beta} - v^{*}_{\alpha\beta}\right)e'_{\alpha\beta}\right] - \frac{R}{L}Q^{nov} + \omega P\,. \tag{16}$$

3 Design of predictive-DPC based on duty cycle control

3.1 Principle of the method

Fig. 2 shows the block diagram of the proposed method. At the start of each switching interval, the rectifier phase voltages and line currents are measured and transformed into the two-phase plane. The output DC bus voltage is measured and compared to a predefined reference value and transmitted to an IP controller to generate an active power reference value. For operation with unity power factor, the reactive power reference value is set to zero. The predicted values of the active power P^{k+1} and the new reactive power $Q^{nov,k+1}$ for each voltage vector component v^k of the converter are used by the cost function block which compares these predicted values with their reference values P^{ref} and Q^{ref}, to generate the optimal voltage vector components (v_α, v_β). Then the duty cycle block determines the optimal duration t_v of the active vector which must be added to the zero vector during a control period.

Active and reactive powers can be calculated from

$$P^k = \frac{3}{2}\mathrm{Re}\left(i^{*}_{\alpha\beta} \times e_{\alpha\beta}\right) \tag{17}$$

$$Q^{nov,k} = \frac{3}{2}\mathrm{Re}\left(i^{*}_{\alpha\beta} \times e'_{\alpha\beta}\right), \tag{18}$$

where k is the current sampling instant.

The predicted values of the active and reactive powers are given as follows:

$$\frac{dP}{dt} = \frac{P(k+1) - P(k)}{T_s} \tag{19}$$

$$\frac{dQ^{nov}}{dt} = \frac{Q^{nov}(k+1) - Q^{nov}(k)}{T_s}, \tag{20}$$

where T_s is the sampling period and (k + 1) is the next sampling instant.

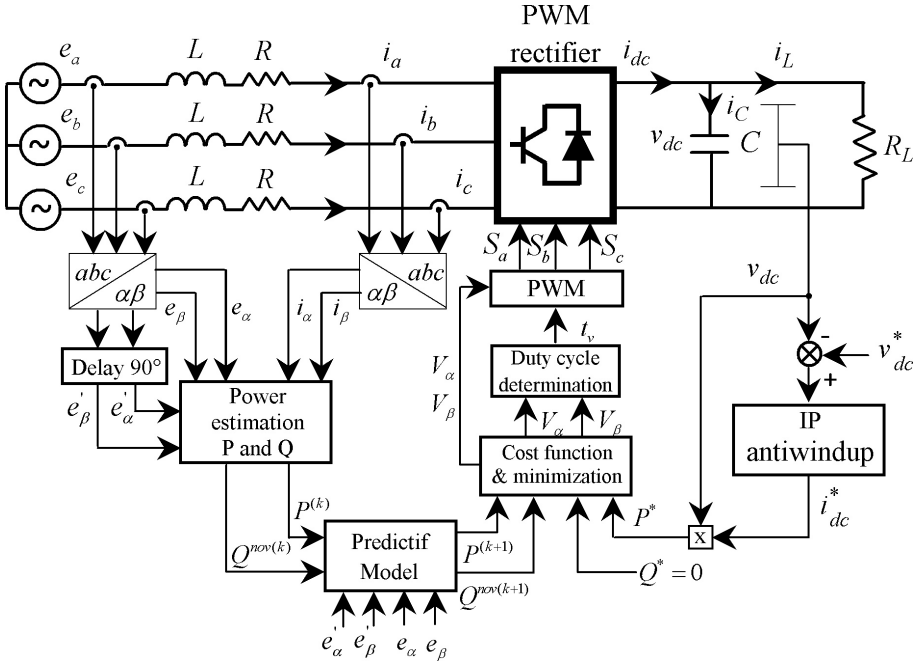

Fig. 2 Control diagram of predictive DPC with duty cycle control under unbalanced grid voltage conditions

By substituting Eqs. (17) and (18) in Eqs. (19) and (20), we will have:

$$\frac{P(k+1)-P(k)}{T_s} = A \tag{21}$$

$$\frac{Q^{nov}(k+1)-Q^{nov}(k)}{T_s} = B\,, \tag{22}$$

where:

$$A = \frac{3}{2L}\left[\left|e^k_{\alpha\beta}\right|^2 - \mathrm{Re}\left(v^{*k}_{\alpha\beta}\times e^k_{\alpha\beta}\right) - \frac{R}{L}P - \omega Q^{nov,k}\right] \tag{23}$$

$$B = \frac{3}{2L}\mathrm{Re}\left[\left(e^{*k}_{\alpha\beta} - v^{*k}_{\alpha\beta}\right)e'^k_{\alpha\beta}\right] - \frac{R}{L}Q^{nov,k} + \omega P^k\,, \tag{24}$$

given that:

$$\begin{cases}\mathrm{Re}\left(v^{*k}_{\alpha\beta}\times e^k_{\alpha\beta}\right) = v_\alpha e_\alpha + v_\beta e_\beta \\ \mathrm{Re}\left[\left(e^{*k}_{\alpha\beta} - v^{*k}_{\alpha\beta}\right)e'^k_{\alpha\beta}\right] = \left(e_\alpha - v_\alpha\right)e'_\alpha + \left(e_\beta - v_\beta\right)e'_\beta\end{cases}, \tag{25}$$

so

$$A = \frac{3}{2L}\left[\left(e^2_\alpha + e^2_\beta\right) - v_\alpha e_\alpha - v_\beta e_\beta\right] - \frac{R}{L}P^k - \omega Q^{nov,k} \tag{26}$$

$$B = \frac{3}{2L}\mathrm{Re}\left[\left(e_\alpha - v_\alpha\right)e'_\alpha + \left(e_\beta - v_\beta\right)e'_\beta\right] - \frac{R}{L}Q^{nov} + \omega P\,. \tag{27}$$

The active and reactive powers at the next sampling instant (k + 1) can be calculated using Eqs. (28) and (29):

$$P^{k+1} = P^k + AT_s \tag{28}$$

$$Q^{nov,k+1} = Q^{nov,k} + BT_s\,. \tag{29}$$

The new cost function is calculated as follows:

$$g = \left(P^{ref} - P^{k+1}\right)^2 + \left(Q^{ref} - Q^{nov,k+1}\right)^2 \tag{30}$$

By replacing Eqs. (28) and (29) in Eq. (30), we get:

$$g = \left(P^{ref} - P^k - AT_s\right)^2 + \left(Q^{ref} - Q^{nov,k} - BT_s\right)^2, \tag{31}$$

where A and B are calculated in Eqs. (26) and (27).

The minimization problem will be solved as follows:

$$\begin{cases}\dfrac{dg}{dv_\alpha} = \dfrac{3T_s}{L}\left(P^{ref} - P^k - AT_s\right)e_\alpha \\ +\dfrac{3T_s}{L}\left(Q^{ref} - Q^{nov,k} - BT_s\right)e'_\alpha = 0 \\ \dfrac{dg}{dv_\beta} = \dfrac{3T_s}{L}\left(P^{ref} - P^k - AT_s\right)e_\beta \\ +\dfrac{3T_s}{L}\left(Q^{ref} - Q^{nov,k} - BT_s\right)e'_\beta = 0\end{cases}. \tag{32}$$

Finally, by solving the system of Eq. (32), the optimal voltage vector components (v_α, v_β) of the converter can be written as follows:

$$\begin{cases}\dfrac{2L}{3T_s}X + \left(e^2_\alpha + e'^2_\alpha\right)v_\alpha + \left(e_\alpha e_\beta + e'_\alpha e'_\beta\right)v_\beta = 0 \\ \dfrac{2L}{3T_s}Y + \left(e_\alpha e_\beta + e'_\alpha e'_\beta\right)v_\alpha + \left(e^2_\beta + e'^2_\beta\right)v_\beta = 0\end{cases} \tag{33}$$

$$\begin{cases} v_\alpha = \dfrac{2L}{3T_s\left(e_\alpha e'_\beta - e'_\alpha e_\beta\right)^2}\left[\left(e_\alpha e_\beta + e'_\alpha e'_\beta\right)Y - \left(e_\beta^2 + e_\beta'^2\right)X\right] \\ v_\beta = -\dfrac{1}{\left(e_\alpha e_\beta + e'_\alpha e'_\beta\right)}\left[\dfrac{2L}{3T_s}X + \left(e_\alpha^2 + e_\alpha'^2\right)v_\alpha\right] \end{cases} \tag{34}$$

with

$$\begin{cases} X = \Delta P e_\alpha - \dfrac{3T_s}{2L}e_\alpha\left(e_\alpha^2 + e_\beta^2\right) + \dfrac{RT_s}{L}e_\alpha P^k + \omega T_s e_\alpha Q^{nov,k} + \ldots \\ +\Delta Q e'_\alpha + \dfrac{RT_s}{L}e'_\alpha Q^{nov,k} - \omega T_s e'_\alpha P^k - \dfrac{3T_s}{2L}e_\alpha e_\alpha'^2 - \dfrac{3T_s}{2L}e_\beta e'_\alpha e'_\beta \\ Y = \Delta P e_\beta - \dfrac{3T_s}{2L}e_\beta\left(e_\alpha^2 + e_\beta^2\right) + \dfrac{RT_s}{L}e_\beta P^k + \omega T_s e_\beta Q^{nov,k} + \ldots \cdot \\ +\Delta Q e'_\beta + \dfrac{RT_s}{L}e'_\beta Q^{nov,k} - \omega T_s e'_\beta P^k - \dfrac{3T_s}{2L}e_\beta e_\beta'^2 - \dfrac{3T_s}{2L}e_\beta e'_\alpha e'_\beta \\ \Delta P = P^{ref} - P^k \\ \Delta Q = Q^{ref} - Q^{nov,k} \end{cases} \tag{35}$$

3.2 Duty cycle control

In order to further reduce the power ripple due to the use of zero voltage vector, we introduce the duty cycle control in the predictive direct power control (P-DPC). In this control technique, the selection of an active vector and a zero vector during a control period is explained as follows. From Fig. 3, it is clearly seen that the zero voltage vector produces much smaller power variations than the other non-zero voltage vectors. Therefore, to obtain a reduction in the power ripple, it is possible to combine the zero voltage vector with the non-zero voltage vector during a control period.

In P-DPC control, the active vector to be applied during a control period is selected by the cost function in Eq. (29) and determined by Eq. (34). Fig. 4 illustrates the changes in active power and new reactive power during a control period when both an active vector and a zero vector are applied. The changes in active power are ρ_1 and ρ_2 for the active voltage vector and the zero voltage vector, and the changes in the new reactive power are ρ_{11} and ρ_{22}, can be easily obtained from Eqs. (23) and (24).

From Fig. 4, the active power and the new reactive power at the next instant (k + 1) can be predicted as follows:

$$P^{k+1} = P^k + \rho_1 t_v + \rho_2\left(t_{sp} - t_v\right) \tag{36}$$

$$Q^{nov,k+1} = Q^{nov,k} + \rho_{11} t_v + \rho_{22}\left(t_{sp} - t_v\right). \tag{37}$$

The optimal duration t_v of the active vector can be obtained by minimizing the cost function Eq. (29) at the next instant.

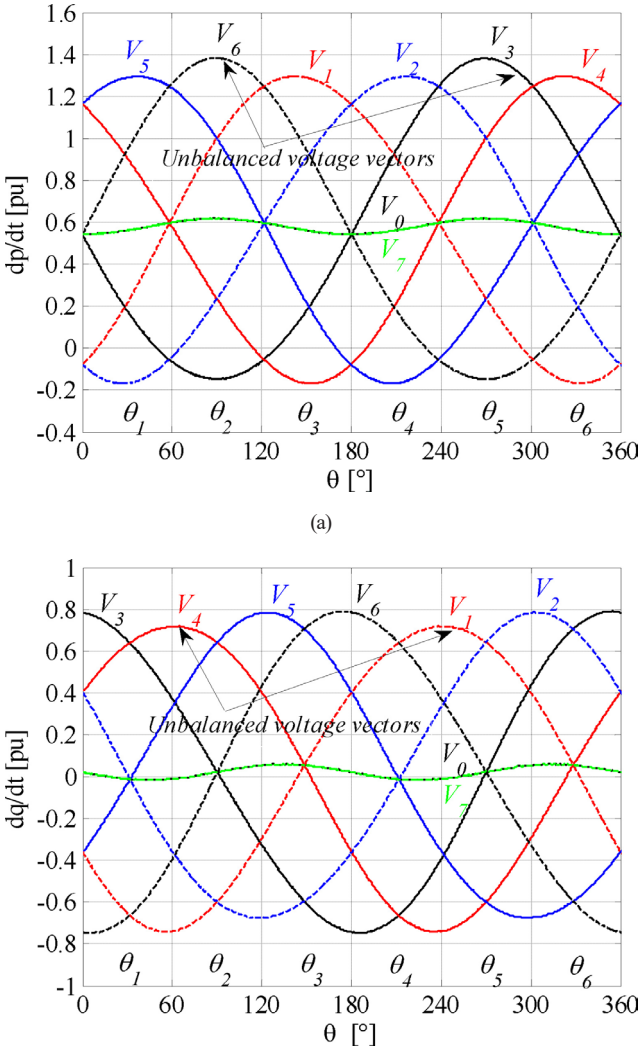

Fig. 3 Slopes of active power (a) and the new reactive power (b) for various rectifier voltage vectors under unbalanced grid voltage conditions

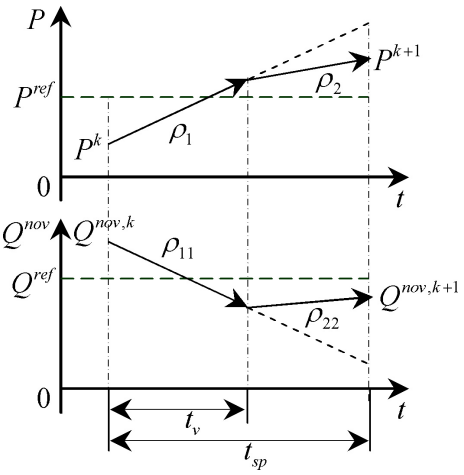

Fig. 4 Active and reactive power variations throughout one control period when applying an active vector and a zero vector

By substituting Eqs. (36) and (37) into Eq. (29) and solving $\frac{\partial g}{\partial t_v}=0$, the optimal duration of the best active vector minimization during a control period is obtained as follows:

$$t_v=\frac{\left(P^{ref}-P^{k+1}\right)\left(\rho_1-\rho_2\right)+\left(Q^{ref}-Q^{nov,k+1}\right)\left(\rho_{11}-\rho_{22}\right)}{\left(\rho_1-\rho_2\right)^2+\left(\rho_{11}-\rho_{22}\right)^2}+\dots$$
$$+\frac{t_{sp}\left(\rho_2^2+\rho_{22}^2-\rho_1\rho_2-\rho_{11}\rho_{22}\right)}{\left(\rho_1-\rho_2\right)^2+\left(\rho_{11}-\rho_{22}\right)^2}. \tag{38}$$

The value of t_v is set to zero if t_v is negative, or t_{sp} if t_v is greater than t_{sp}.

The knowledge of the voltage sector is necessary to determine the optimum switching states. For this, the work frame (α, β) is divided into six sectors as shown in Fig. 5. The number of sectors is determined instantaneously by the position of the voltage vector components given by

$$\theta_n=\arctan\left(\frac{e_\beta}{e_\alpha}\right);\ n=1,\dots,6. \tag{39}$$

During a control period, the active vectors obtained by the P-DPC are applied for the optimal duration t_v, followed by the appropriate zero vectors with minimal switching steps. Taking the following rules, vectors $\left(\vec{V}_2,\vec{V}_4,\vec{V}_6\right)$ must be followed by vector $\vec{V}_7$, while other vectors $\left(\vec{V}_1,\vec{V}_3,\vec{V}_5\right)$, must be followed by vector $\vec{V}_0$.

4 Simulation results

The new predictive DPC control approach using duty cycle control, based on the previous relationships, has been implemented on MATLAB/Simulink software,

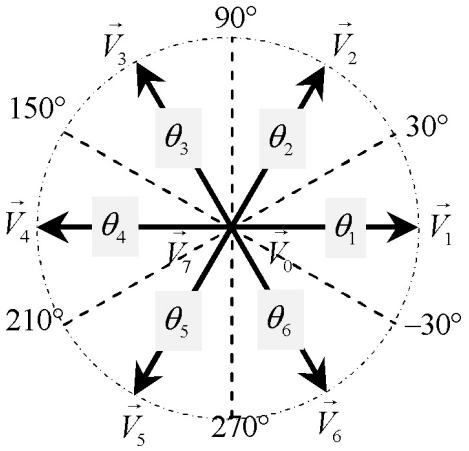

Fig. 5 Vector diagram of PWM rectifier

Fig. 6. The simulation was run under the same unbalanced grid voltage conditions and with the same parameters of the PWM rectifier used in the conventional and improved DPC control, Table 1. The simulation results are given in Fig. 7.

The difference between the two DPC controls namely the improved DPC and the proposed P-DPC lies in the robustness and the ability to keep the ideal trajectories despite the disturbances imposed by the unbalanced network. In this simulation test, the magnitude of the negative sequence voltage vector is assumed to be 10% of the positive sequence voltage vector at t = 0.4 s, Fig. 7 (a). It can be seen that when the network is unbalanced in the case of the predictive-DPC, the three-phase currents of the network exhibit a quasi-sinusoidal waveform and significantly better than those presented in the case of the improved DPC, Fig. 7 (b). We notice the same remark for the currents in the $\alpha\beta$ axes, Fig. 7 (c). We also notice that the unbalanced network does not affect the stability and the regulation of the DC bus voltage of the predictive-DPC with the duty cycle control, Fig. 7 (d). To compare the effect of the same disturbance on the improved DPC and the proposed predictive-DPC, we use the normalized error of the DC output voltage produced by the disturbance on the two DPC controls. It is noticed that the normalized error is almost zero for the two structures, namely proposed predictive-DPC and improved DPC, unlike the conventional DPC, Fig. 7 (e). This shows that the proposed predictive DPC also offers good DC voltage control during voltage unbalance. Fig. 7 (f) shows that the grid current is in phase with the grid voltage in the case of the proposed predictive-DPC, thus providing unity power factor. The predictive-DPC control adjusts well the active power in all sectors when the load power decreases, Fig. 7 (g). It is clearly seen in Fig. 7 (h), that the reactive power is held at zero in order to obtain unity power factor. There is a significant attenuation of the active and reactive power ripples in the case of the predictive-DPC control. It can be clearly seen that the predictive-DPC also achieves decoupled control of active and reactive powers and remains insensitive to voltage unbalance, which shows that the proposed analytical approach is quite rigorous.

The grid current harmonic spectrum for conventional DPC, improved DPC and proposed P-DPC under unbalanced grid voltage conditions, is shown in more detail in Fig. 7 (i). It is clearly seen that the current is highly distorted in the conventional DPC (Fig. 7 (b)) and the THD

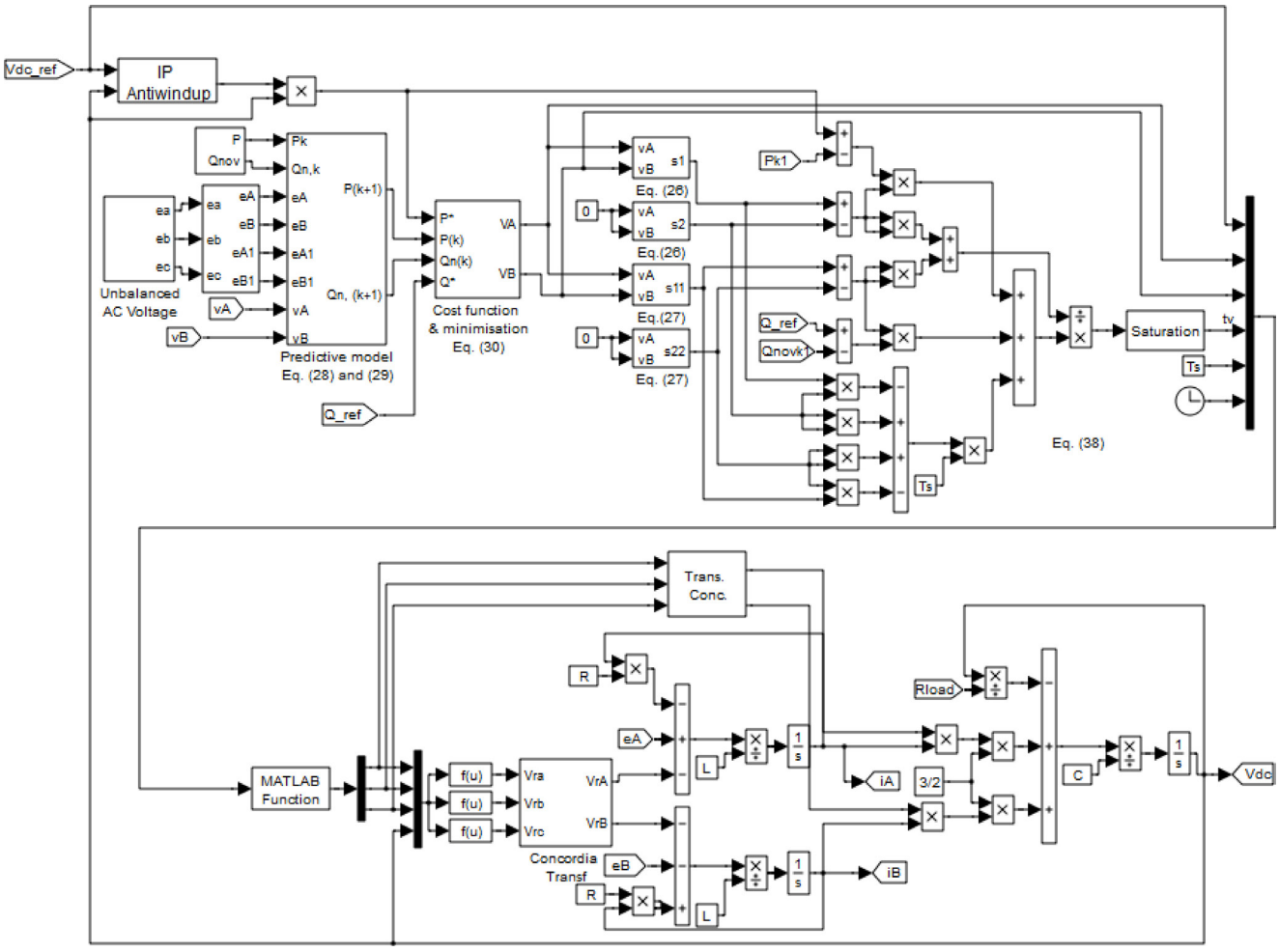

Fig. 6 Simulink model of predictive-DPC based on duty cycle control of PWM rectifier under unbalanced network

Table 1 Rectifier parameters

The input phase voltage:	$V = 125$ V / $f = 50$ Hz
The input inductance:	$L = 37$ mH
The input resistance:	$R = 0.3$ Ω
The output capacitor:	$C_{dc} = 1100$ µF
The output voltage:	$V_{dc} = 350$ V

reaches 8.95%. On the contrary, the THD in improved DPC is only 3.90% after using the new definition of reactive power as the control variable. A THD in proposed P-DPC is as low as 2.56%, which is much lower than the results obtained by the other DPC controls. Finally, simulation results show that predictive-DPC using duty cycle control brings improvement on system performance and robustness compared to conventional DPC and improved DPC during voltage unbalance.

5 Conclusion

In this work, we presented the predictive direct power control (P-DPC) strategy using duty cycle control for a two-level PWM rectifier under unbalanced grid voltage conditions. To compensate simultaneously the DC bus unbalance and grid unbalance, while improving the power factor, P-DPC control has been applied to control the PWM rectifier, where it is possible to predict the behavior of the system at each sampling instant for different control actions, and to choose the most optimal vector to apply it to the system at the next instant. In the studied P-DPC control using the duty cycle control method, the duration of the selected active vector is obtained based on the principle of minimizing the active power ripple during a control period. Simulation results show that this control strategy achieves reduced power ripples and lower current THD while maintaining higher and faster dynamic response than conventional DPC. Moreover, it offers an improvement on the waveform of the absorbed currents and a significant regulation of the active and reactive instantaneous powers and the DC bus voltage.

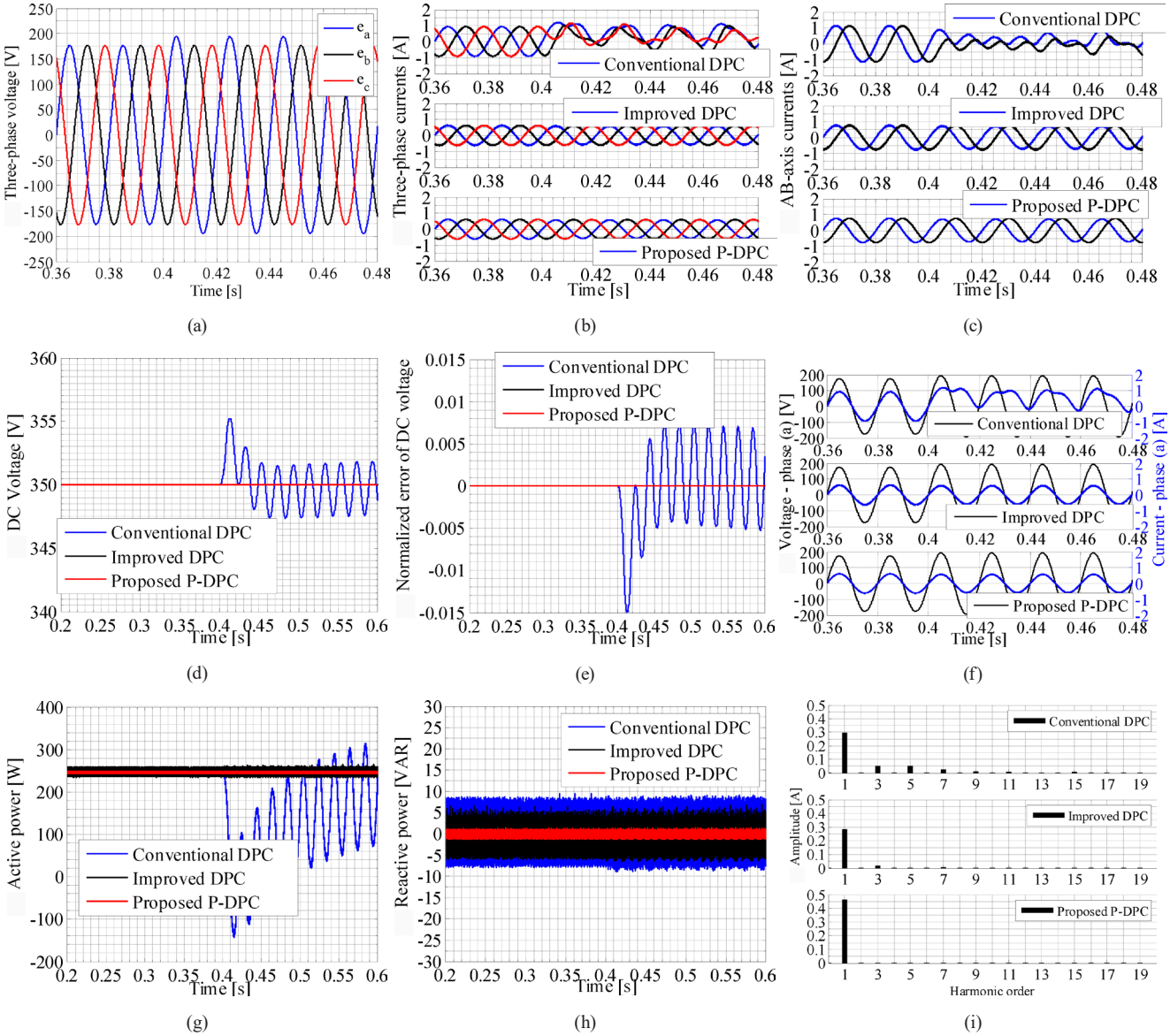

Fig. 7 Simulation results

References

[1] Collier, D. A. F., Heldwein, M. L. "Modeling and design of a micro wind energy system with a variable-speed wind turbine connected to a permanent magnet synchronous generator and a PWM rectifier", In: XI Brazilian Power Electronics Conference, Natal, Brazil, 2011, pp. 292–299. https://doi.org/10.1109/COBEP.2011.6085301

[2] Wu, B., Chen, H., Guan, G., Ding, T., Yin, L. "Simulation model of three-phase PWM rectifier charging station and harmonic analysis on grid", In: 2017 IEEE Innovative Smart Grid Technologies - Asia (ISGT-Asia), Auckland, New Zealand, 2017, pp. 1–6. https://doi.org/10.1109/ISGT-Asia.2017.8378340

[3] Zhang, Y., Jin, L., Jing, Y., Zhao, Z., Lu, T. "Three-Level PWM Rectifier Based High Efficiency Batteries Charger for EV", In: 2013 IEEE Vehicle Power and Propulsion Conference (VPPC), Beijing, China, 2013, pp. 1–4. https://doi.org/10.1109/VPPC.2013.6671722

[4] Zhang, Y., Qu, C. "Model Predictive Direct Power Control of PWM Rectifiers Under Unbalanced Network Conditions", IEEE Transactions on Industrial Electronics, 62(7), pp. 4011–4022, 2015. https://doi.org/10.1109/TIE.2014.2387796

[5] Zhang, Y., Peng, Y., Qu, C. "Model Predictive Control and Direct Power Control for PWM Rectifiers with Active Power Ripple Minimization", IEEE Transactions on Industry Applications, 52(6), pp. 4909–4918, 2016. https://doi.org/10.1109/TIA.2016.2596240

[6] Hartani, K., Miloud, Y. "Control Strategy for Three Phase Voltage Source PWM Rectifier Based on the Space Vector Modulation", Advances in Electrical and Computer Engineering, 10(3), pp. 61–65, 2010. https://doi.org/10.4316/aece.2010.03010

[7] Hang, L., Liu, S., Yan, G., Qu, B., Lu, Z. "An Improved Deadbeat Scheme With Fuzzy Controller for the Grid-side Three-Phase PWM Boost Rectifier", IEEE Transactions on Power Electronics, 26(4), pp. 1184–1191, 2011. https://doi.org/10.1109/TPEL.2010.2089645

[8] Bobrowska-Rafał, M., Rafał, K., Abad, G., Jasiński, M. "Control of PWM rectifier under grid voltage dips", Bulletin of the Polish Academy of Sciences: Technical Sciences, 57(4), pp. 337–343, 2009. https://doi.org/10.2478/v1075-010-0136-x

[9] Reyes, M., Rodriguez, P., Vazquez, S., Luna, A., Teodorescu, R., Carrasco, J. M. "Enhanced Decoupled Double Synchronous Reference Frame Current Controller for Unbalanced Grid-Voltage Conditions", IEEE Transactions on Power Electronics, 27(9), pp. 3934–3943, 2012. https://doi.org/10.1109/TPEL.2012.2190147

[10] Reyes, M., Rodríguez, P., Vázquez, S., Luna, A., Carrasco, J. M., Teodorescu, R. "Decoupled Double Synchronous Reference Frame current controller for unbalanced grid voltage conditions", In: 2012 IEEE Energy Conversion Congress and Exposition (ECCE), Raleigh, NC, USA, 2012, pp. 4676–4682. https://doi.org/10.1109/ECCE.2012.6342184

[11] Noguchi, T., Tomiki, H., Kondo, S., Takahashi, I. "Direct power control of PWM converter without power-source voltage sensors", IEEE Transactions on Industry Applications, 34(3), pp. 473–479, 1998. https://doi.org/10.1109/28.673716

[12] Chikouche, T. M., Hartani, K. "Direct Power Control of Three-phase PWM Rectifier Based on New Switching Table", Journal of Engineering Science and Technology, 13(6), pp. 1751–1763, 2018. [online] Available at: http://jestec.taylors.edu.my/Vol%2013%20issue%206%20June%202018/13_6_27.pdf [Accessed: 27 June 2018]

[13] Bouafia, A., Gaubert, J.-P., Krim, F. "Predictive Direct Power Control of Three-Phase Pulsewidth Modulation (PWM) Rectifier Using Space-Vector Modulation (SVM)", IEEE Transactions on Power Electronics, 25(1), pp. 228–236, 2010. https://doi.org/10.1109/TPEL.2009.2028731

[14] Zhang, Y., Li, Z., Zhang, Y., Xie, W., Piao, Z., Hu, C. "Performance Improvement of Direct Power Control of PWM Rectifier With Simple Calculation", IEEE Transactions on Power Electronics, 28(7), pp. 3428–3437, 2013. https://doi.org/10.1109/TPEL.2012.2222050

[15] Zhang, Y., Xie, W., Li, Z., Zhang, Y. "Model Predictive Direct Power Control of a PWM Rectifier With Duty Cycle Optimization", IEEE Transactions on Power Electronics, 28(11), pp. 5343–5351, 2013. https://doi.org/10.1109/TPEL.2013.2243846

[16] Suh, Y., Lipo, T. A. "Modeling and analysis of instantaneous active and reactive power for PWM AC/DC converter under generalized unbalanced network", IEEE Transactions on Power Delivery, 21(3), pp. 1530–1540, 2006. https://doi.org/10.1109/TPWRD.2005.860274

[17] Chikouche, T. M., Hartani, K., Nasri, S. E., Ameur, A. E. "Improved Direct Power Control of PWM Rectifier under Unbalanced Network based on new Power Reactive Estimation", In: 2021 12th International Symposium on Advanced Topics in Electrical Engineering (ATEE), Bucharest, Romania, 2021, pp. 1–7. https://doi.org/10.1109/ATEE52255.2021.9425051

[18] Karamanakos, P., Pavlou, K., Manias, S. "An Enumeration-Based Model Predictive Control Strategy for the Cascaded H-Bridge Multilevel Rectifier", IEEE Transactions on Industrial Electronics, 61(7), pp. 3480-3489, 2014. https://doi.org/10.1109/TIE.2013.2278965

[19] Zhang, Y., Qu, C. "Direct Power Control of a Pulse Width Modulation Rectifier Using Space Vector Modulation Under Unbalanced Grid Voltages", IEEE Transactions on Power Electronics, 30(10), pp. 5892–5901, 2015. https://doi.org/10.1109/TPEL.2014.2371469

[20] Zhang, Y., Xie, W., Li, Z., Zhang, Y. "Low-Complexity Model Predictive Power Control: Double-Vector-Based Approach", IEEE Transactions on Industrial Electronics, 61(11), pp. 5871–5880, 2014. https://doi.org/10.1109/TIE.2014.2304935

[21] Yan, S., Chen, J., Yang, T., Hui, S. Y. "Improving the Performance of Direct Power Control Using Duty Cycle Optimization", IEEE Transactions on Power Electronics, 34(9), pp. 9213–9223, 2019. https://doi.org/10.1109/TPEL.2018.2883425

[22] Tai, L., Lin, M., Li, H., Li, Y. "A Novel Three-Vector-Based Model Predictive Direct Power Control for Three-Phase PWM Rectifier", Electronics, 10(21), Article number: 2579, 2021. https://doi.org/10.3390/electronics10212579